DISCRETE AND CONTINUOUS
DYNAMICAL SYSTEMS SERIES B

doi:10.3934/dcdsb.2020004

ON THE ABEL DIFFERENTIAL EQUATIONS OF THIRD KIND

Regilene Oliveira*

Departamento de Matemática, ICMC-Universidade de São Paulo
Avenida Trabalhador São-carlense, 400,
13566-590, São Carlos, SP, Brazil

Cláudia Valls

Departamento de Matemática, Instituto Superior Técnico
Universidade Técnica de Lisboa, Av. Rovisco Pais
1049–001, Lisboa, Portugal

(Communicated by Miguel Sanjuan)

Abstract. Abel equations of the first and second kind have been widely studied, but one question that never has been addressed for the Abel polynomial differential systems is to understand the behavior of its solutions (without knowing explicitly them), or in other words, to obtain its qualitative behavior. This is a very hard task that grows exponentially as the number of parameters in the equation increases. In this paper, using Poincaré compactification we classify the topological phase portraits of a special kind of quadratic differential system, the Abel quadratic equations of third kind. We also describe the maximal number of polynomial solutions that Abel polynomial differential equations can have.

1. **Introduction and statement of the main results.** Generalized polynomial Abel differential equations of the form

$$C(x)y^m\dot{y} = A(x) + B(x)y \tag{1}$$

(here the dot denotes derivative with respect to the independent variable x and $m \geq 0$), appear in all textbooks of ordinary differential equations as examples of nonlinear equations and in many mathematical and applied problems, see [10, 13, 14] and the references therein.

If $m = 0$ or $m = 1$ equations (1) become the well-known Abel equations of the first and second kind that have been widely studied. Here we will focus in the case in which $m = 2$, known as Abel equations of the third kind, and when the functions A, B, C are polynomials in x. More precisely we will work with the polynomial differential equations

$$C(x)y^2\frac{dy}{dx} = A(x) + B(x)y, \tag{2}$$

or equivalently to the polynomial differential system

$$\begin{aligned}\dot{x} &= c(x)y^2,\\ \dot{y} &= a(x) + b(x)y,\end{aligned}$$

2010 *Mathematics Subject Classification.* Primary: 37C15, 37C10.

Key words and phrases. Abel polynomial differential equations, vector fields, phase portraits, polynomial solutions.

* Corresponding author.

where $A(x) = a(x)/c(x)$, $B(x) = b(x)/c(x)$, $C(x) = c(x)$, and the dot denotes derivative with respect to the independent variable t.

The first motivation of this paper comes from works about the existence of polynomial solutions for another kind of polynomial differential systems that appears in applied problems known as Riccati differential systems. Such systems can be written as $a(x)\dot{y} = b_0(x) + b_1(x)y + b_2(x)y^2$, where a, b_0, b_1 and b_2 are polynomial in the variable x and many papers about them can be found. For instance, Rainville [14] proved the existence of one or two polynomial solutions for a subclass of such systems. Bhargava and Kaufman [2, 3] obtained some sufficient conditions for such equations to have polynomial solutions. Campbell and Golomb [4, 5] provided some criteria determining the degree of polynomial solutions of such equations. Bhargava and Kaufman [1] also considered a more general form of such equations and got some criteria on the degree of polynomial solutions of the equations. Giné, Grau and Llibre [9] proved that polynomial differential equations of the form $a(x)\dot{y} = b_0(x) + b_1(x)y + .. + b_n(x)y^n$ with $n \geq 1$, $b_i(x) \in \mathbb{R}[x]$, $i = 0, 1, ..., n$ and $b_n(x) = 0$ and $a(x) = 1$ have at most n polynomial solutions and they also prove that this bound is sharp. More recently, Gasull, Torregrosa and Zhang in [7] proved that the maximum number of polynomial solutions of the equations studied in [9] when $a(x)$ is nonconstant is $n+1$ when $n \geq 1$ and these bounds are sharp. In short, to be best of our knowledge, the question of knowing the maximum number of polynomial solutions of some polynomial differential equations like (1) when $C(x)$ is nonconstant is open. This is also interesting because it is similar to a question of Poincaré about the degree and number of algebraic solutions of autonomous planar polynomial differential equations in terms of their degrees, when these systems have finitely many algebraic solutions.

The first theorem of the paper is the following.

Theorem 1.1. *The following statements hold for the Abel polynomial differential equation of third kind (2) with $C \not\equiv 0$ and either $A \not\equiv 0$ or $B \not\equiv 0$.*

(a) it has at most 1 constant solution and there are examples with exactly 1 constant solution.

(b) If it has a polynomial solution then it has infinitely many polynomial solutions.

The proof of Theorem 1.1 is given in Section 2.

Another question that never has been addressed for the Abel polynomial differential systems is to understand the behavior of its solutions (without knowing explicitly them), or in other words, to obtain its qualitative behavior. This is a very hard task that grows exponentially as the number of parameters in the equation increases. This is the reason why in our second main result among the Abel polynomial differential systems of third kind, we will focus on the quadratic ones. The Abel quadratic differential polynomial systems of third kind are of the form

$$\begin{aligned} \dot{x} &= cy^2, \\ \dot{y} &= a_0 + a_1x + a_2x^2 + (b_0 + b_1x)y, \end{aligned} \tag{3}$$

where $c \neq 0$ and $a_0, a_1, a_2, b_0, b_1, b_2$ are real parameters with $a_0^2 + a_1^2 + a_2^2 \neq 0$. We will obtain the phase portraits of the polynomial vector fields $\mathcal{X}$ here studied and will be given in the Poincaré disk $\mathcal{D}$, see Chapter 5 of [6] for the definition of the Poincaré disk and the expressions of the compactified polynomial vector fields $p(\mathcal{X})$ in the local charts U_1 and U_2 of $\mathcal{D}$ that we shall use in the computations.

We say that two polynomial vector fields $p(\mathcal{X})$ and $p(\mathcal{Y})$ in the Poincaré disk are *topologically equivalent* if there exists a homeomorphism from one onto the

other sending orbits to orbits preserving or reversing the direction of the flow. The *separatrix configuration* of $p(\mathcal{X})$ is formed by all the separatrices of $p(\mathcal{X})$ plus an orbit in each one of its canonical regions. Recall that a *canonical region* is a connected component of the Poincaré disk after removing from it all the separtrices of the vector field. Moreover, if $p(\mathcal{X})$ and $p(\mathcal{Y})$ are two compactified Poincaré polynomial vector fields with finitely many separatrices, then they are topologically equivalent if and only if their separatrix configurations are homeomorphic (see [12] for a proof). This last result will be used for obtaining the phase portraits in the Poincaré disk of our polynomial differential system (3).

Our second main result is the following one.

Theorem 1.2. *The Abel quadratic polynomial differential equations* (3) *after a linear change of variables and a rescaling of its independent variable can be written as one of the following systems*

$$\dot{x} = y^2, \quad \dot{y} = k_0 + k_1 y + x^2 + k_2 xy \qquad k_0, k_2 \in \mathbb{R} \quad \text{and} \quad k_1 \in \{0, 1\}, \tag{i}$$

$$\dot{x} = y^2, \quad \dot{y} = x + k_1 y + k_2 xy \qquad k_1 \in \mathbb{R} \quad \text{and} \quad k_2 \in \{-1, 0, 1\}, \tag{ii}$$

$$\dot{x} = y^2, \quad \dot{y} = 1 + k_2 xy \qquad k_2 \in \{-1, 1\}, \tag{iii}$$

$$\dot{x} = y^2, \quad \dot{y} = 1 + k_1 y \qquad k_1 \in \{0, 1\}. \tag{iv}$$

Moreover, the global phase portraits on the Poincaré disk of these families are topologically equivalent to the following ones in Figures 1, 2 and 3. More precisely, for system (i) *the phase portraits are*

(1) when $k_0 > 0$ *and* $k_2 < 3/4^{1/3}$;
(2) when $k_0 > 0$ *and* $k_2 = 3/4^{1/3}$;
(3) when $k_0 > 0$ *and* $k_2 > 3/4^{1/3}$;
(4) when $k_0 = 0$ *and* $k_2 < 3/4^{1/3}$;
(5) when $k_0 = 0$ *and* $k_2 = 3/4^{1/3}$;
(6) when $k_0 = 0$ *and* $k_2 > 3/4^{1/3}$;
(7) when $k_0 = k_1 = 0$ *and* $k_2 < 3/4^{1/3}$;
(8) when $k_0 = k_1 = 0$ *and* $k_2 = 3/4^{1/3}$;
(9) when $k_0 = k_1 = 0$ *and* $k_2 > 3/4^{1/3}$;
(10)–(12) when $k_0 < 0$, $k_2 < 3/4^{1/3}$, $k_1 + \sqrt{-k_0}k_2 > 0$ *and* $k_1 - \sqrt{-k_0}k_2 > 0$;
(13)–(17) when $k_0 < 0$, $k_2 < 3/4^{1/3}$, $k_1 + \sqrt{-k_0}k_2 < 0$ *and* $k_1 - \sqrt{-k_0}k_2 > 0$;
(19) when $k_0 < 0$, $k_2 < 3/4^{1/3}$, $k_1 + \sqrt{-k_0}k_2 > 0$ *and* $k_1 - \sqrt{-k_0}k_2 < 0$;
(19)–(21) when $k_0 < 0$, $k_2 = 3/4^{1/3}$, $k_1 + \sqrt{-k_0}k_2 > 0$ *and* $k_1 - \sqrt{-k_0}k_2 > 0$;
(22)–(26) when $k_0 < 0$, $k_2 = 3/4^{1/3}$, $k_1 + \sqrt{-k_0}k_2 > 0$ *and* $k_1 - \sqrt{-k_0}k_2 < 0$;
(27)–(29) when $k_0 < 0$, $k_2 > 3/4^{1/3}$, $k_1 + \sqrt{-k_0}k_2 > 0$ *and* $k_1 - \sqrt{-k_0}k_2 > 0$;
(30)–(34) when $k_0 < 0$, $k_2 > 3/4^{1/3}$, $k_1 + \sqrt{-k_0}k_2 > 0$ *and* $k_1 - \sqrt{-k_0}k_2 < 0$;
(35) when $k_0 < 0$ *and* $k_1 = k_2 = 0$;
(36) when $k_0 < 0$ *and either* $k_1 = -\sqrt{-k_0 k_2}$ *and* $k_2 \neq 0$, *or* $k_1 = \sqrt{-k_0 k_2}$ *and* $k_2 < 3/4^{1/3}$;
(37) and (38) when $k_0 < 0$, $k_1 = -\sqrt{-k_0 k_2}$ *and* $k_2 \neq 0$;
(39) when $k_0 < 0$, $k_1 = \sqrt{-k_0 k_2}$ *and* $k_2 = 3/4^{1/3}$;
(40) when $k_0 < 0$, $k_1 = \sqrt{-k_0 k_2}$ *and* $k_2 > 3/4^{1/3}$;

For system (ii) *the phase portraits are*

(4) when $k_1 \neq 0$ *and* $k_2 \in \{-1, 0\}$;
(6), (43) and (44) when $k_1 \neq 0$ *and* $k_2 = 1$;
(41) when $k_1 = 0$ *and* $k_2 \in \{-1, 0\}$;

(42) when $k_1 = 0$ and $k_2 = 1$;

For system (iii) the phase portrait is

(1) when $k_2 = -1$;

(3) when $k_2 = 1$;

For system (iv) the unique phase portrait is (1);

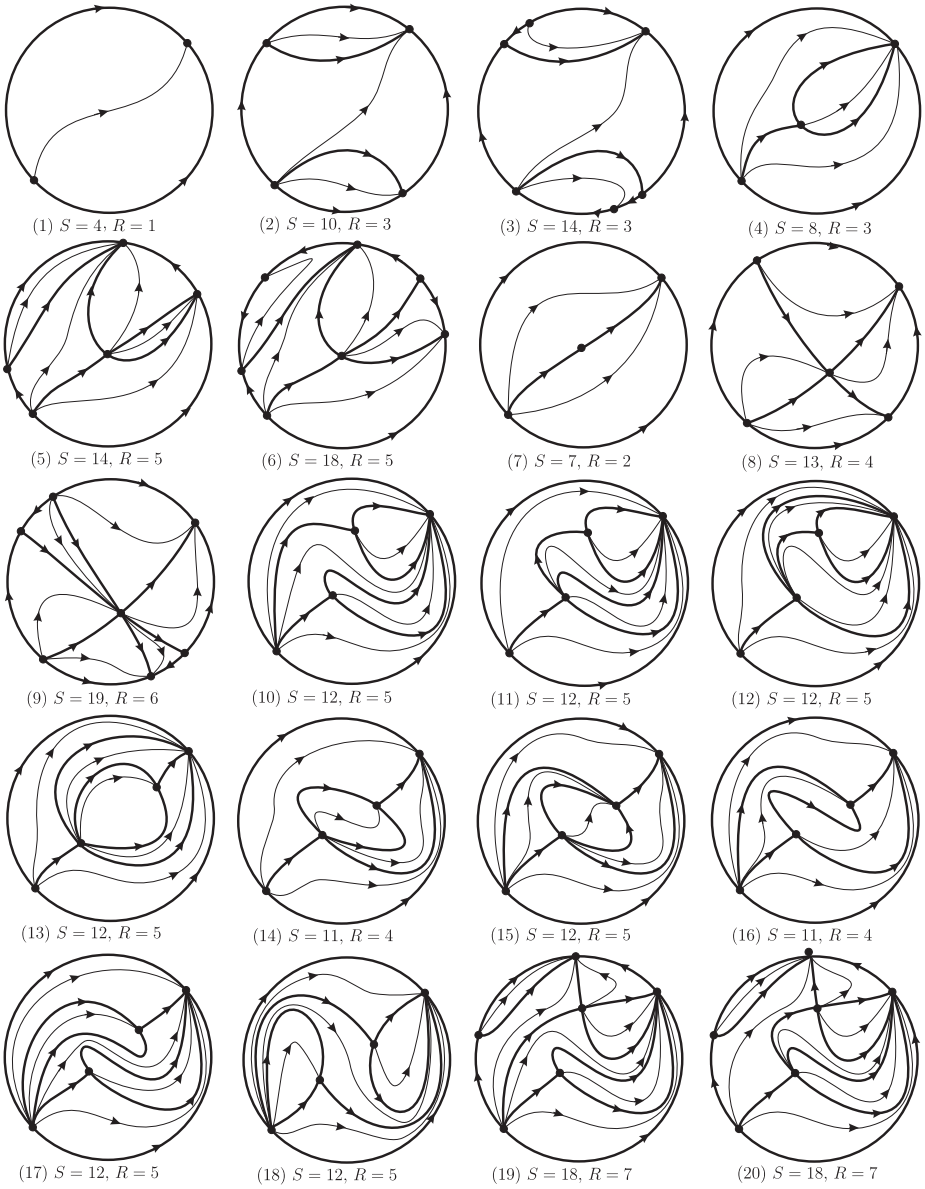

FIGURE 1. Global phase portraits in the Poincaré disk of systems (i)–(iv): from (1)–(20). Here S denotes the number of separatrices and R the number of canonical region of each phase portrait.

The proof of Theorem 1.2 will be given in Sections 3–6.

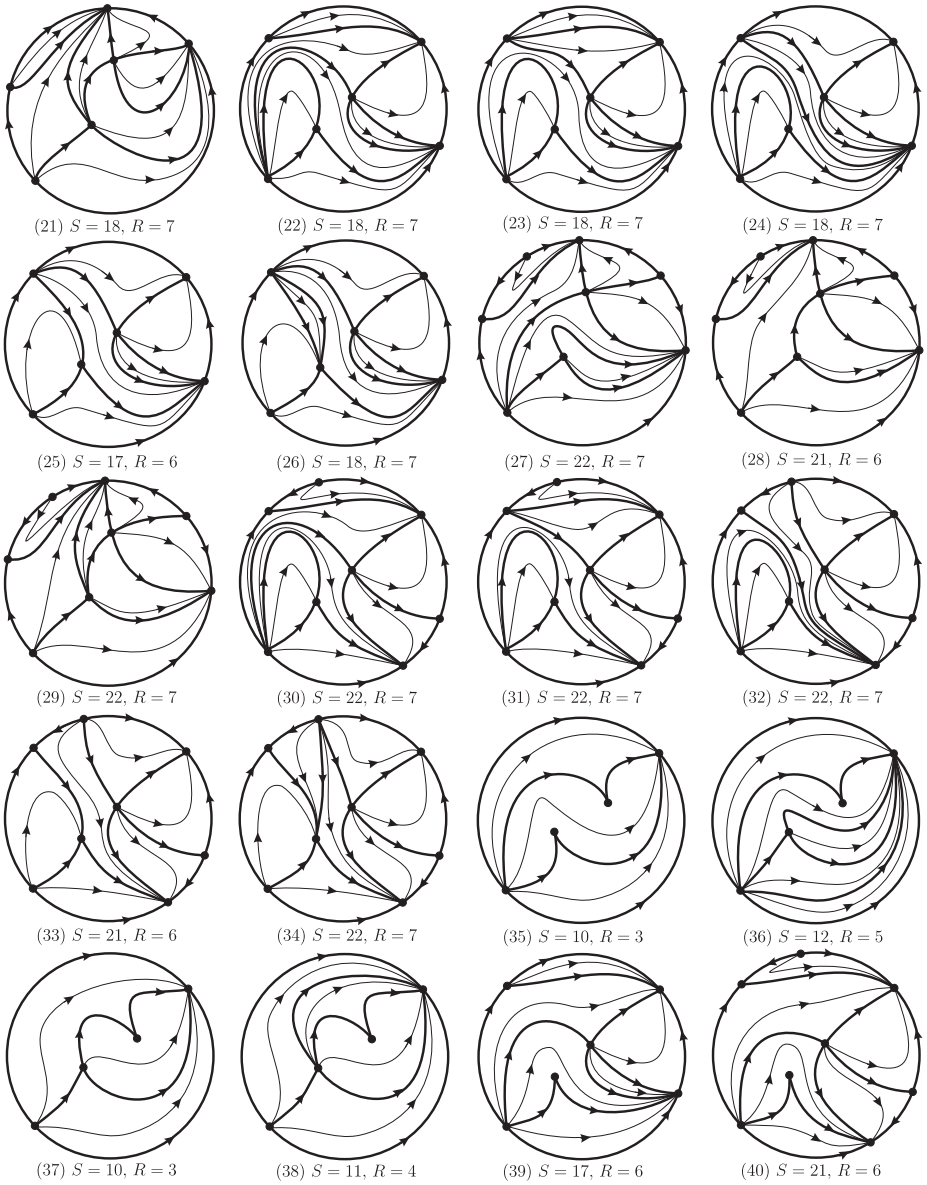

FIGURE 2. Global phase portraits in the Poincaré disk of systems (i)–(ii): from (21)–(40). Here S denotes the number of separatrices and R the number of canonical region of each phase portrait.

2. **Proof of Theorem 1.1.** Let $y = p(x) = \xi$ be a polynomial solution of system (2) which is constant. As either $A \not\equiv 0$ or $B \not\equiv 0$ the polynomial in y, $A(x) + B(x)y$ is divisible by $y - \xi$ and, since its degree in y is 1, we get that it has at most 1 different constant root. So, there is at most 1 different constant solution of system (2). The differential equation

$$C(x)y^2 \frac{dy}{dx} = y - 1$$

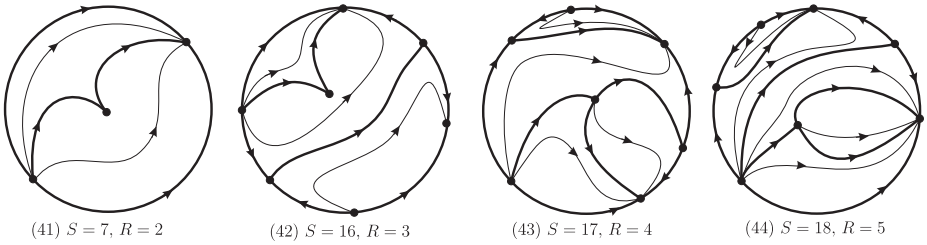

FIGURE 3. Global phase portraits in the Poincaré disk of systems (ii): from (41)–(44). Here S denotes the number of separatrices and R the number of canonical region of each phase portrait.

is of the form (2) and has exactly 1 constant solution. This proves statement (a).

Now we prove statement (b). Let $y = p(x)$ be a polynomial solution of system (2) which is not a constant, that is,

$$C(x)p(x)^2\frac{dp}{dx} = b_0(x) + b_1(x)p + b_2(x)p^2.$$

Since p divides the left-hand side of the above equation, it must also divide the right-hand side and so $A(x) = \tilde{A}(x)p(x)$ for some polynomial $\tilde{A}(x)$. In this way equation (2) becomes

$$C(x)p\frac{dp}{dx} = \overline{A}(x) + B(x).$$

Note that p still divides the left-hand side of the above equation and so it must also divide the right-hand side, which means that $\overline{A}(x) + B(x) = A^*(x)p(x)$ for some polynomial A^*. Hence, we have

$$C(x)\frac{dp}{dx} = A^*(x).$$

Clearly $C(x)$ must divide $A^*(x)$ and so we must have $A^*(x) = C(x)\tilde{A}(x)$, for some polynomial $\tilde{A}(x)$. Hence,

$$p(x) = \int \tilde{A}(s)\,ds + c,$$

where c is any constant. This proves statement (b).

3. **Normal forms given in Theorem 1.2.** In this section we describe the normal forms given in Theorem 1.2, that is, systems (i)–(iv).

Proposition 1. *An Abel quadratic polynomial differential system (3) after a linear change of variables and a rescaling of its independent variable, can be written as (i), (ii), (iii), or (iv).*

Proof. Doing a linear change of variables and a rescaling of the independent variable (the time) of the form $x \to \alpha X + \sigma, y \to \beta Y, t \to \gamma T$, with $\beta\delta\gamma \neq 0$, system (3) becomes

$$\begin{aligned}\dot{X} =& cY^2\beta^2\gamma/\alpha,\\ \dot{Y} =& b_0Y\gamma + b_1XY\alpha\gamma + (a_0\gamma)/\beta + (a_1X\alpha\gamma)/\beta + (a_2X^2\alpha^2\gamma)/\beta + b_1Y\gamma\sigma + (a_1\gamma\sigma)/\beta\\ &+ (2a_2X\alpha\gamma\sigma)/\beta + (a_2\gamma\sigma^2)/\beta,\end{aligned}$$

where the dot denotes derivative with respect to the new time T.

Since $c \neq 0$ we take $\alpha = c\beta^2\gamma$. Now we consider different cases.

If $a_2 \neq 0$ we take $\sigma = -a_1/(2a_2)$ and $\gamma = 1/(a_2^{1/3}c^{2/3}\beta)$ so we get system (i) with $k_0 = -((a_1^2 - 4a_0a_2)/(4a_2^{4/3}c^{2/3}\beta^2)), k_1 = (2a_2b_0 - a_1b_1)/(2a_2^{4/3}c^{2/3}\beta)$ and $k_2 = b_1/(a_2^{2/3}c^{1/3})$. Note that if $2a_2b_0 = a_1b_1 = 0$ then $k_1 = 0$, otherwise we can take $\beta = 2a_2^{4/3}c^{2/3}/(2a_2b_0 - a_1b_1)$ and we get $k_1 = 0$. In short, we get system (i) with $k_1 \in \{0, 1\}$.

If $a_2 = 0$ and $a_1 \neq 0$ we take $\sigma = -a_0/a_1, \beta = 1/(a_1c\gamma^2)$ and we get system (ii) with $k_1 = (a_1b_0 - a_0b_1)\gamma/a_1$ and $k_2 = b_1/(a_1^2c\gamma^2)$. Note that if $b_1 = 0$ then $k_2 = 0$. Otherwise taking $\gamma = \sqrt{b_1/(a_1^2c)}$ if $b_1c > 0$, or $\gamma = \sqrt{-b_1/(a_1^2c)}$ if $b_1c < 0$ we get system (ii) with $k_2 \in \{-1, 0, 1\}$.

If $a_2 = a_1 = 0$ then $a_0 \neq 0$. If $b_1 \neq 0$ we take $\sigma = -b_0/b_1$ and $\gamma = \beta/a_0$ and we get system (iii) with $k_2 = b_1c\beta^4/a_0^2$. Moreover, note that $k_2 \neq 0$ because $b_1 \neq 0$ and taking $\beta = (a_0^2/(b_1c))^{1/4}$ if $b_1c > 0$ or $\beta = (-a_0^2/(b_1c))^{1/4}$ if $b_1c < 0$ we get that $k_2 \in \{-1, 1\}$.

On the other hand, if $b_1 = 0$ then taking $\gamma = \beta/a_0$ we get system (iv) with $k_1 = b_0\beta/a_0$. Note that if $b_0 = 0$ then $k_1 = 0$ and if $b_0 \neq 0$ then taking $\beta = a_0/b_0$ we get $k_1 = 1$. In short, we obtain system (iv) with $k_1 \in \{0, 1\}$. This concludes the proof of the proposition. □

4. **Global behavior of system (i) of Theorem 1.2.** In this section we describe the global phase portraits of system (i). We will separate the proof in different subsections. First we study the finite and infinite singular points and then we joint the obtained information to describe the distinct global phase portraits.

If $k_0 > 0$ there are no finite singular points. If $k_0 = 0$ the unique finite singular point is the origin and if $k_0 < 0$ there are two finite singular points which are $(\sqrt{-k_0}, 0)$ and $(-\sqrt{-k_0}, 0)$.

If $k_0 < 0$ and $(k_1 + \sqrt{-k_0}k_2)(k_1 - \sqrt{-k_0}k_2) \neq 0$ they are semi–hyperbolic and using Theorem 2.19 in [6] both of them are saddle-nodes. If $k_0 < 0$, $k_1 + \sqrt{-k_0} = 0$ and $k_1 - \sqrt{-k_0} \neq 0$ then $(\sqrt{-k_0}, 0)$ is nilpotent and $(-\sqrt{-k_0}, 0)$ is semi–hyperbolic. Using Theorems 3.5 and 2.19 in [6] we conclude that $(\sqrt{-k_0}, 0)$ is a cusp and $(-\sqrt{-k_0}, 0)$ is a saddle-node. If $k_0 < 0$, $k_1 + \sqrt{-k_0} \neq 0$ and $k_1 - \sqrt{-k_0} = 0$ then $(-\sqrt{-k_0}, 0)$ is nilpotent and $(\sqrt{-k_0}, 0)$ is semi–hyperbolic. Using Theorems 3.5 and 2.19 in [6] we conclude that $(-\sqrt{-k_0}, 0)$ is a cusp and $(\sqrt{-k_0}, 0)$ is a saddle-node. If $k_0 < 0$ and $k_1 = k_2 = 0$ then both $(\pm\sqrt{-k_0}, 0)$ are nilpotent and by Theorem 3.5 in [6] we get that they are both cusps.

If $k_0 = 0$ and $k_1 = 1$ the origin is the unique finite singular point. It is semi–hyperbolic. Applying Theorem 2.19 in [6] we conclude that it is a saddle-node. If $k_0 = k_1 = 0$ the origin is again the unique finite singular point which in this case is linearly zero. Applying a blow up in the direction $(x, y) \to (x, w)$ where $w = y/x$ and a rescaling $ds = xdt$, we get the following system

$$\begin{aligned} \dot{x} = &\quad w^2x \\ \dot{w} = &\quad 1 + k_2w - w^3. \end{aligned}$$

This system either has one or three singular points (counted with multiplicities). These singular points are of the form $(0, w)$ where w is a real root of $1+k_2w-w^3 = 0$. The discriminant of the cubic equation is $4k_2^3 - 27$. If $k_2 < 3/4^{1/3}$ there is a unique real solution (positive) which is hyperbolic. If $k_2 = 3/4^{1/3}$ there are two real solutions, $w = -1/2^{1/3}$ (a saddle-node) and $w = 2^{2/3}$ (a saddle). If $k_2 > 3/4^{1/3}$ there are three real different solutions that are hyperbolic. To study the topological type of these solutions we will study the polynomial $f(w) = 1 + k_2w - w^3$. If

$k_2 < 0$ then f is strictly decreasing and intersects the w-axes in a unique point (the real root of $1 + k_2 w - w^3$). The eigenvalues of the Jacobian matrix at the point $(0, w)$ are w^2 and $k_2 - 3w^2$. Note that at this root $w \neq 0$ and $k_2 - 3w^2 < 0$, so this point is a saddle. If $k_2 > 0$ then f has a maximum at $w = \sqrt{k_2/3}$ and a minimum at $w = -\sqrt{k_2/3}$. If $k_2 \in (0, 3/4^{1/3})$ then $f(-\sqrt{k_2/3})$ and $f(\sqrt{k_2/3})$ are both positive. Since $\lim_{w\to\infty} f(w) = -\infty$ and $\lim_{w\to-\infty} f(w) = \infty$, we get that f intersects the w-axes in a unique point (the real root). Again by the eigenvalues of the Jacobian matrix at this point we get that it is a saddle. If $k_2 > 3/4^{1/3}$ then $f(-\sqrt{k_2/3})$ is negative and $f(\sqrt{k_2/3})$ is positive. Since $\lim_{w\to\infty} f(w) = -\infty$ and $\lim_{w\to-\infty} f(w) = \infty$ we get that f intersects the w-axes in three points w_0, w_1 and w_2 (the real roots), where $w_0 < -\sqrt{k_2/3}$, $w_1 \in -\sqrt{k_2/3}, \sqrt{k_2/3})$ and $w_2 > \sqrt{k_2/3}$. Again by the eigenvalues of the Jacobian matrix at these points we get that w_0 and w_2 are saddles and w_1 is an unstable node.

Doing the blowing down we get that when $k_2 < 3/4^{1/3}$ the origin is formed by two hyperbolic sectors and when $k_2 \geq 3/4^{1/3}$ it is formed by the union of two hyperbolic sectors separated by parabolic sectors. See Figure 4 for details about the blowing down.

Remark 1. Note that $\dot{x} > 0$ for $y \neq 0$ and $\dot{y}|_{(x_0,0)} < 0$ for $x_0 \in (-\sqrt{-k_0}, \sqrt{-k_0})$. This will help when studying the global behavior of the solutions. Moreover, $\dot{y} = 0$ yields the nullcline curve $y = -(x^2 + k_0)/(k_1 + k_2 x)$. The nulllcline curve separates the phase portrait in two regions such that above it, $\dot{y}$ is positive and below it, $\dot{y}$ is negative.

To study the singular points at infinity of a polynomial vector field via the Poincaré compactification we need to study the singular points in the local chart U_1 and the origin of the local chart U_2.

The Poincaré compactification $p(\mathcal{X})$ of system (i) in the local chart U_1 is given by

$$\begin{aligned} \dot{u} = &\quad 1 + k_2 u - u^3 + k_1 uv + k_0 v^2, \\ \dot{v} = &\quad -u^2 v. \end{aligned}$$

The singular points in the local chart U_1 are $(u, 0)$ where u is a root of the polynomial $1 + k_2 u - u^3$. The same study that we did for the finite singular points when $k_0 = k_1 = 0$ taking into account that the eigenvalues of the Jacobian matrix at the singular points $(u, 0)$ are $-u^2$ and $k2 - 3u^2$ we get: if $k_2 < 3/4^{1/3}$ there is a unique singular point in the local chart U_1 which is a stable node, if $k_2 = 3/4^{1/3}$ there are two singular point in the local chart U_1 which are $(-1/2^{1/3}, 0)$ (a saddle–node) and $(2^{1/3}, 0)$ (a stable node), and if $k_2 > 3/4^{1/3}$ there are three singular points in the local chart U_1 which are $(u_0, 0), (u_1, 0)$ and $(u_2, 0)$ with $u_0 < -\sqrt{k_2/3}$, $u_1 \in (-\sqrt{k_2/3}, \sqrt{k_2/3})$ and $u_2 > \sqrt{k_2/3})$, being $(u_0, 0), (u_2, 0)$ stable nodes and $(u_1, 0)$ a saddle.

System (i) in the local chart U_2 is written as

$$\begin{aligned} \dot{u} = &\quad 1 - k_2 u^2 - u^3 - k_1 uv - k_0 uv^2, \\ \dot{v} = &\quad -k_2 uv - u^2 v - k_1 v^2 - k_0 v^3. \end{aligned}$$

So the origin of the local chart U_2 is not an infinite singular point.

4.1. **Global phase portraits for system (i) with $k_0 > 0$.** If $k_0 > 0$ there are no finite singular points, that is, it is a chordal quadratic system (see [8]). If $k_2 < 3/4^{1/3}$ there is a unique stable node in the local chart U_1 and using Remark

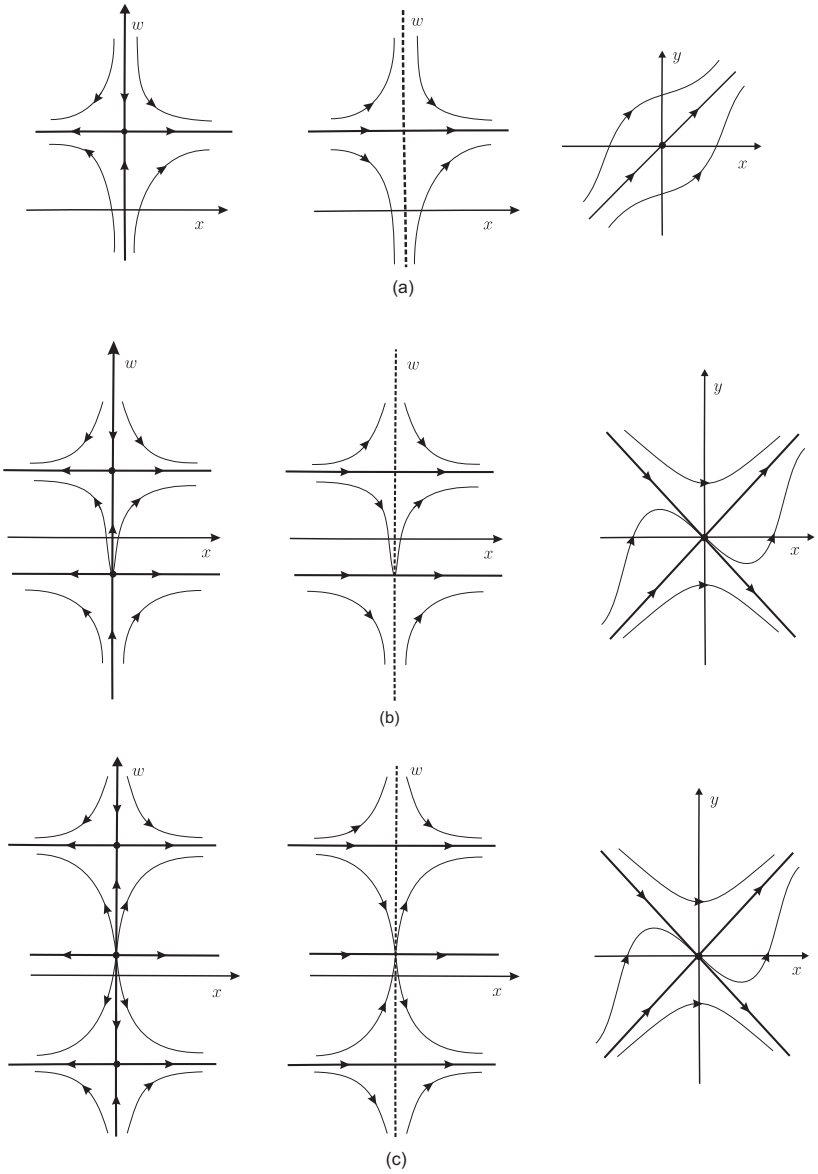

FIGURE 4. Blowing down process for system (i) at origin when $k_0 = k_1 = 0$ and $k_2 < 3/4^{1/3}$ (a), $k_2 = 3/4^{1/3}$ (b), and $k_2 > 3/4^{1/3}$ (c)

1 we get that the unique possible global phase portrait is (1) of Figure 1. This phase portrait is topologically equivalent to 8 in [8], where it is described all the possible global phase portrait for chordal quadratic polynomial differential systems. As described in [8] when there is a unique stable node in the local chart U_1 there is a unique phase portrait. If $k_2 = 3/4^{1/3}$ then we have two singular points in

the local chart U_1, a saddle-node and a stable node. In this case the global phase portrait is (2) of Figure 1. This is due the fact that $\dot{y}|_{y=0} = x^2 + k_0 > 0$. This corresponds to 5 in [8]. Although in [8] there are more possible configurations the fact that $\dot{y}|_{y=0} = x^2 + k_0 > 0$ prevent them here. If $k_2 > 3/4^{1/3}$ there are three singular points in the local chart U_1, a saddle and two stable nodes. Again using that $\dot{y}|_{y=0} = x^2 + k_0 > 0$ we get that the unique global phase portrait is (3) of Figure 1. This corresponds to 1 in [8]. As in the previous case although in [8] there are more possible configurations the fact that $\dot{y}|_{y=0} = x^2 + k_0 > 0$ prevent them here.

4.2. **Global phase portraits for system** (i) **with** $k_0 = 0$ **and** $k_1 = 1$**.** In this case there is a unique singular point, the origin which is a saddle–node. Using that $\dot{y}|_{y=0} = x^2 + k_0 > 0$ and $\dot{x}|_{y=0} = 0$ we have a unique possible global phase portrait for each of the cases depending on whether in the local chart U_1 we have a unique stable node, a saddle-node and a stable node, or a saddle and two stable nodes. In short we have phase portrait (4) of Figure 1 (when $k_2 < 3/4^{1/3}$), phase portrait (5) of Figure 1 (when $k_2 = 3/4^{1/3}$) and phase portrait (6) of Figure 1 (when $k_2 > 3/4^{1/3}$).

4.3. **Global phase portraits for system** (i) **with** $k_0 = k_1 = 0$**.** In this case there is a unique singular point, the origin, which is formed by two hyperbolic sectors if $k_2 < 3/4^{1/3}$, and by two hyperbolic sectors separated by parabolic sectors if $k_2 \geq 3/4^{1/3}$. Taking into account the information on the local chart U_1, that $\dot{y}|_{y=0} = x^2 + k_0 > 0$ and that $\dot{x}|_{y=0} = 0$, we conclude that the unique possible global phase portraits are (7) of Figure 1 (when $k_2 < 3/4^{1/3}$), (8) of Figure 1 (when $k_2 = 3/4^{1/3}$) and (9) of Figure 1 (when $k_2 > 3/4^{1/3}$).

4.4. **Global phase portraits for system** (i) **with** $k_0 < 0$**,** $k_2 < 3/4^{1/3}$ **and** $(k_1 + \sqrt{-k_0}k_2)(k_1 - \sqrt{-k_0}k_2) \neq 0$**.** As explained above in this case we have two finite saddle–nodes at $(\pm\sqrt{-k_0}, 0)$ and a stable node in the local chart U_1. The position of the separatrix of these saddle-nodes depend on whether $k_1 + \sqrt{-k_0}k_2 > 0$ or $k_1 + \sqrt{-k_0}k_2 < 0$ and $k_1 - \sqrt{-k_0}k_2 > 0$ or $k_1 - \sqrt{-k_0}k_2 < 0$. So we will separate our study in three cases (we recall that $k_1 \in \{0, 1\}$):

Case 1: $k_1 + \sqrt{-k_0}k_2 > 0$ and $k_1 - \sqrt{-k_0}k_2 > 0$;
Case 2: $k_1 + \sqrt{-k_0}k_2 < 0$ and $k_1 - \sqrt{-k_0}k_2 > 0$;
Case 3: $k_1 + \sqrt{-k_0}k_2 > 0$ and $k_1 - \sqrt{-k_0}k_2 < 0$.

Taking into account the first statement in Remark 1 and that in Case 1 the two saddle–nodes are as in Figure 5 (a), the unique possible global phase portraits are (10)–(12) of Figure 1. Phase portrait (10) is attained, for example, when $k_0 = -1/2, k_1 = 1, k_2 = 1/2$ and phase portrait (12) when $k_0 = -1/2, k_1 = 1, k_2 = -1/2$. Phase portrait (11) corresponds to the separatrix connexion and its existence comes from the continuity of the parameters.

In Case 2 the two saddle-nodes are as in Figure 5 (b). Again using the first statement in Remark 1 we get that the possible global phase portraits are (13)-(17) of Figure 1 depending on the relative position of the separatrizes of the two saddle–nodes. Phase portrait (13) is attained when $k_0 = -1, k_1 = 1, k_2 = -2$ and phase portrait (15) when $k_0 = -1, k_1 = 0, k_2 = -2$. Phase portrait (17) is attained when $k_0 = -1, k_1 = 0, k_2 = -1$. By continuity of the parameters we get phase portraits (14) and (16) which correspond to separatrix connections.

In Case 3 the two saddle-nodes are as in Figure 5 (c). Again using the first statement in Remark 1 we conclude that the unique global phase portrait is (18) of Figure 1 which is attained for example when $k_0 = -1, k_1 = 0$ and $k_2 = 14/10$.

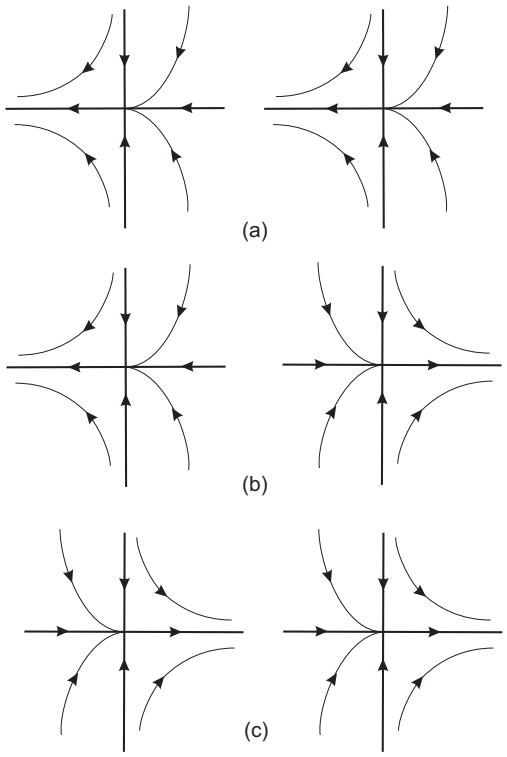

FIGURE 5. The position of the separatrices of the two saddle-nodes $(\pm\sqrt{-k_0}, 0)$ for system (i) with $k_0 < 0$, $k_2 < 3/4^{1/3}$ and $(k_1 + \sqrt{-k_0}k_2)(k_1 - \sqrt{-k_0}k_2) \neq 0$

4.5. **Global phase portraits for system (i) with $k_0 < 0$, $k_2 = 3/4^{1/3}$ and $(k_1 + \sqrt{-k_0}k_2)(k_1 - \sqrt{-k_0}k_2) \neq 0$.** We will separate again our study in the three cases above. Note that the statement about the nullcline in Remark 1 forces that the α-limit of the separatrix of the saddle–node at infinity must be the finite point $(\sqrt{-k_0}, 0)$.

The argument above together with the first statement in Remark 1 imply that the possibilities of the global behavior of the solutions in Case 1 is limited to phase portraits (19) and (20) of Figure 1 and, (21) of Figure 2. Phase portrait (19) is attained at $k_0 = -3/20, k_1 = 1$ and phase portrait (21) at $k_0 = -2/25, k_1 = 1$. As in the previous subsection, phase portrait (20) corresponds to the separatrix connection and it is realized due to the continuity of the parameters. We recall that phase portraits (10)–(12) of Figure 1 correspond to the case in which the two infinity singular points at the local chart U_1 coalesce.

The argument at the beginning of this subsection together with the first statement in Remark 1 forbids the existence of global phase portraits in Case 2.

The same arguments as in the above subsection imply that in Case 3, the possible global phase portraits are (22)–(26) of Figure 2. Phase portrait (22) is attained at

$k_0 = -14/5, k_1 = 1$, phase portrait (24) at $k_0 = -1, k_1 = 1/2$, and phase portrait (26) at $k_0 = -3, k_1 = 0$. Phase portraits (23) and (25) correspond to the separatrix connections and they are realized due to the continuity of the parameters.

4.6. **Global phase portraits for system** (i) **with** $k_0 < 0$, $k_2 > 3/4^{1/3}$ **and** $(k_1 + \sqrt{-k_0}k_2)(k_1 - \sqrt{-k_0}k_2) \neq 0$**.** Again we separate our study in three cases. Note that the statement about the nullcline in Remark 1 forces that the α-limit of the separatrix of the saddle at infinity must be the separatrix of the finite singular point $(\sqrt{-k_0}, 0)$. This information together with the first statement in Remark 1 imply that the possibilities of the global behavior of the solutions in Case 1 is limited to phase portraits (27)–(29) of Figure 2. Phase portrait (27) is attained at $k_0 = -1/20, k_1 = 1, k_2 = 39/10$ and phase portrait (29) at $k_0 = -1/8, k_1 = 1, k_2 = 2$. Phase portrait (28) is the separatrix connection and it is realized due to the continuity of the parameters. We remark that phase portraits (19) and (20) of Figure 1 and, (21) of Figure 2 correspond to the case in which the saddle and stable node in the local chart U_1 coalesce.

As in the previous subsection for Case 2 there are no possible global phase portraits.

In Case 3 the possible global phase portraits are (30)–(34) of Figure 2. Phase portrait (30) is attained at $k_0 = -1/2, k_1 = 1, k_2 = 2$, phase portrait (32) at $k_0 = -1, k_1 = 1, k_2 = 2$ and phase portrait (34) at $k_0 = -1, k_1 = 0, k_2 = 2$. Phase portraits (31) and (33) correspond to separatrix connections and they are realized due to the continuity of the parameters. We remark that phase portraits (22)–(26) of Figure 2 correspond to the case in which the saddle and stable node in the local chart U_1 coalesce.

4.7. **Global phase portraits for system** (i) **with** $k_0 < 0$ **and** $k_1 = -\sqrt{-k_0}k_2$**.** Since $k_1 \in \{0, 1\}$ we get that $k_2 \leq 0$. This implies that in the local chart U_1 we have a unique stable node. Moreover, the finite singular point $(\sqrt{-k_0}, 0)$ is a cusp. If $k_2 \neq 0$ the finite singular point $(-\sqrt{-k_0}, 0)$ is a saddle-node and if $k_2 = 0$ it is a cusp. We remark that the phase portraits of quadratic systems with a finite cusp were studied by Jager in [11]. Here, using Remark 1 we get that the unique global phase portraits are (36)–(38) of Figure 2 when $k_2 \neq 0$ and phase portrait (35) of Figure 2 when $k_2 = 0$. Phase portrait (36) is attained when $k_0 = -2, k_2 = -1/2$ and it is topologically equivalent to phase portrait 4 of Figure 14 in [11]. Phase portrait (38) is attained when $k_0 = -1, k_2 = -1$ and is topologically equivalent to phase portrait 1 of Figure 14 in [11]. Phase portrait (37) corresponds to the separatrix connection, is realized due to the continuity of the parameters and is topologically equivalent to phase portrait 2 of Figure 14 in [11].

4.8. **Global phase portraits for system** (i) **with** $k_0 < 0$, $k_1 = \sqrt{-k_0}k_2$ **and** $k_2 \neq 0$**.** In this case $k_2 > 0$ (the case $k_1 = k_2 = 0$ is given in subsection 4.7). The explanation about the nullclines and the first statement in Remark 1 yield that the unique global phase portraits are (36) of Figure 2 when $k_2 < 3/4^{1/3}$ (there is a unique stable node in the local chart U_1), (39) of Figure 2 when $k_2 = 3/4^{1/3}$ (there is a stable node and a saddle-node in the local chart U_1) and (40) of Figure 2 when $k_2 > 3/4^{1/3}$ (there are two stable nodes and a stable node in the local chart U_1). Phase portrait (39) is topologically equivalent to phase portrait 7 of Figure 15 in [11] and phase portrait (40) is topologically equivalent to phase portrait 7 of Figure 16 in [11].

From the previous subsections we conclude the global study of system (i) of Theorem 1.2.

5. **Global behavior of system** (ii) **of Theorem 1.2.** System (ii) has the origin as the unique critical point. The eigenvalues of the Jacobian matrix at the origin are 0 and k_1. So, it is semi-hyperbolic if $k_1 \neq 0$ and nilpotent if $k_1 = 0$. Applying Theorems 2.19 and 3.5 from [6] we get that the origin is a saddle-node if $k_1 \neq 0$ and a cusp if $k_1 = 0$.

The Poincaré compactification $p(\mathcal{X})$ of system (ii) in the local chart U_1 is given by

$$\begin{aligned} \dot{u} = &\quad k_2 u - u^3 + v + k_1 uv, \\ \dot{v} = &\quad -u^2 v. \end{aligned}$$

If $k_2 \in \{-1, 0\}$ the unique singular point in the local chart U_1 is the origin. If $k_2 = 1$ the singular points in the local chart U_1 are $p_1 = (-\sqrt{k_2}, 0), p_2 = (0, 0)$ and $p_3 = (\sqrt{k_2}, 0)$.

If $k_2 = -1$ the origin is a semi-hyperbolic stable node, if $k_2 = 0$ the origin is a nilpotent stable node, and if $k_2 = 1$ the origin is a semi-hyperbolic saddle and the points p_1 and p_3 are hyperbolic stable nodes.

System (ii) in the local chart U_2 is written as

$$\begin{aligned} \dot{u} = &\quad 1 - k_2 u^2 - k_1 uv - u^2 v, \\ \dot{v} = &\quad -k_2 uv - k_1 v^2 - uv^2. \end{aligned}$$

So the origin of the local chart U_2 is not an infinite singular point.

5.1. **Global phase portraits for system** (ii) **with** $k_2 \in \{-1, 0\}$**.** Taking into account that the unique infinite singular point is the origin of the local chart U_1, which is a stable node, and that the origin is the unique finite singular point (either a saddle-node or a cusp), we conclude that the unique possible global phase portraits are (4) of Figure 1 (when $k_1 \neq 0$) and (41) Figure 3 (when $k_1 = 0$).

5.2. **Global phase portraits for system** (ii) **with** $k_2 = 1$**.** If $k_1 = 0$ the unique possible global phase portrait is (42) of Figure 3. If $k_1 \neq 0$ there are three possible global phase portraits according to the $\omega-$ limit of the separatrix of the finite saddle–node. They are (6) of Figure 1 and, (43) and (44) of Figure 3. Phase portrait (6) is attained, for example when $k_1 = -2$ and phase portrait (44) when $k_1 = -1/2$. Phase portrait (43) corresponds to the separatrix connection and it is realized due to the continuity of the parameter k_1.

From the previous subsections we conclude the global study of system (ii) of Theorem 1.2.

6. **Global behavior of systems** (iii) **and** (iv) **of Theorem 1.2.** Systems (iii) and (iv) do not have finite singular points so they are chordal quadratic systems.

The Poincaré compactification $p(\mathcal{X})$ of system (iii) in the local chart U_1 is given by

$$\dot{u} = k_2 u - u^3 + v^2, \qquad \dot{v} = -u^2 v.$$

If $k_2 = -1$ the unique singular point in the local chart U_1 is the origin which is a semi–hyperbolic unstable node. If $k_2 = 1$ there are three infinity singular points which are $(0, 0)$ (a semi-hyperbolic saddle) and $(0, \pm 1)$ which are stable nodes.

System (iii) in the local chart U_2 is written as

$$\dot{u} = 1 - k_2 u^2 - uv^2, \qquad \dot{v} = -k_2 uv - v^3.$$

So the origin of the local chart U_2 is not an infinite singular point.

When $k_2 = -1$ the unique global phase portrait is (1) of Figure 1 and when $k_2 = 1$ the unique global phase portrait is (3) of Figure 1.

The Poincaré compactification $p(\mathcal{X})$ of system (iv) in the local chart U_1 is given by

$$\dot{u} = -u^3 + k_1 uv + v^2, \qquad \dot{v} = -u^2 v,$$

and in the local chart U_2 by

$$\dot{u} = 1 - k_1 uv - uv^2, \qquad \dot{v} = -k_1 v^2 - v^3.$$

The unique infinite singular point is the origin of the local chart U_1 which is a linearly zero stable node, so the unique global phase portrait is (1) of Figure 1.

The proof of Theorem 1.2 comes from Sections 3–6.

Acknowledgments. The authors wish to thank the referee for his/her suggestions which have improved the final version of this paper. The first author is partially supported by FAPESP project number 2017/20854-5. The second author is partially supported by FCT/Portugal through UID/MAT/ 04459/2013.

REFERENCES

[1] M. Bhargava and H. Kaufman, Degrees of polynomial solutions of a class of Riccati-type differential equations, *Collect. Math.*, **16** (1964), 211–223.
[2] M. Bhargava and H. Kaufman, Existence of polynomial solutions of a class of Riccati-type differential equations, *Collect. Math.*, **17** (1965), 135–143.
[3] M. Bhargava and H. Kaufman, Some properties of polynomial solutions of a class of Riccati-type differential equations, *Collect. Math.*, **18** (1966/1967), 3–6.
[4] J. G. Campbell, A criterion for the polynomial solutions of a certain Riccati equation, *Amer. Math. Monthly*, **59** (1952), 388–389.
[5] J. G. Campbell and M. Golomb, On the polynomial solutions of a Riccati equation, *Amer. Math. Monthly*, **61** (1954), 402–404.
[6] F. Dumortier, J. Llibre and J. C. Artés, *Qualitative Theory of Planar Differential Systems*, UniversiText, Springer-verlag, Berlin, 2006.
[7] A. Gasull, J. Torregrosa and X. Zhang, The number of polynomial solutions of polynomial Riccati equations, *J. Differential Equations*, **261** (2016), 5071–5093.
[8] A. Gasull, L.-R. Sheng and J. Llibre, Chordal quadratic systems, *Rocky Mountain J. Math.*, **16** (1986), 751–782
[9] J. Giné, M. Grau and J. Llibre, On the polynomial limit cycles of polynomial differential equations, *Israel J. Math.*, **181** (2011), 461–475.
[10] E. Hille, *Ordinary Differential Equations in the Complex Domain*, Dover Publications, Inc., NY, 1997.
[11] P. de Jager, Phase portraits for quadratic systems with a higher order singularity with two zero eigenvalues, *J. Differential Equations*, **87** (1990), 169–204.
[12] D. A. Neumann, Classification of continuous flows on 2-manifolds, *Proc. Amer. Math. Soc.*, **48** (1975), 73–81.
[13] M. Pollicott, H. Wang and H. Weiss, Extracting the time-dependent transmission rate from infection data via solution of an inverse ODE problem, *J. Biol. Dyn.*, **6** (2012), 509–523.
[14] E. D. Rainville, Necessary conditions for polynomial solutions of certain Riccati equations, *Amer. Math. Monthly*, **43** (1936), 473–476.

Received December 2018; revised May 2019.

E-mail address: regilene@icmc.usp.br
E-mail address: cvalls@math.ist.utl.pt